

# Design of Elliptical Dielectric Resonator Antennas Using Genetic Algorithm and Rayleigh-Ritz Technique

<sup>1</sup>A. Tadjalli, <sup>1</sup>A. Sebak, <sup>2</sup>T. Denidni, and <sup>3</sup>I. Ahadi-Akhlaghi

<sup>1</sup>ECE Dept, Concordia University, Montreal, QC, H3G 1M8, Canada

a\_tadjal@ece.concordia.ca, abdo@ece.concordia.ca

<sup>2</sup>INRS-EMT, 800 de la Gauchetiere, Montreal, QC, H5A 1K6, Canada

<sup>3</sup>ECE Dept, Ferdowsi University, Mashhad, Iran

**Abstract** – In this paper, a specialized genetic algorithm (GA) combined with Rayleigh-Ritz method is used to obtain the dimensions of elliptical dielectric resonators (EDRs) for dual-band, wide-band, or circular polarization (CP) operation. Slot-coupled elliptical dielectric resonator antennas (EDRA's) and their characteristics are investigated. Parametric studies are presented to study the dependence of the return loss on the slot parameters. These parametric studies are used to optimize the slot dimensions and its position to excite given desired modes.

## I. INTRODUCTION

Dielectric Resonators (DR's) have traditionally been used in many applications, such as microwave devices and antennas. Open dielectric resonators are potentially useful antenna elements [1]. Indeed, they offer several attractive features such as small size, high radiation efficiency [1-3], compatibility with MIC's, intrinsic mechanical simplicity, and the ability to obtain different radiation patterns using different modes. Many of the concepts used in the design of microstrip antennas can also be used in the design of dielectric resonator antennas. Dielectric resonator antennas (DRA's) have many similarities with microstrip antennas, such as small size, many possible shapes, lightweight, and ease of feeding with different excitation mechanisms. In addition, several modes can be excited, and each mode has different radiation characteristics. Dielectric resonator antennas have also some advantages over microstrip antennas, such as a wider bandwidth, higher radiation efficiency, wider range of dielectric materials, more geometrical parameters, and higher power capabilities. Systematic experimental investigations on dielectric resonator antennas (DRA's) have first been carried out by Long *et al.* [4-6]. Since then, theoretical and experimental investigations have been reported by many investigators on DRA's of various shapes such as spherical, cylindrical (or cylindrical ring), rectangular, etc. [7-14].

Generating dual-band operation, wide-band operation, and circular polarization (CP) using DRA's are other reasons of their attractiveness for antenna designers.

Recently more attention has focused on the circularly polarized DRA's [10] since it allows a more flexible orientation for both the transmitter and receiver. Generation of CP requires two orthogonal modes in a phase-quadrature signal. Circular polarizations can be obtained using multiple feeds or by alternating the shape of conventional DRA's. The main advantage of single-feed circularly polarized DRA's is their simple structures that do not require an external polarizer.

The application of genetic algorithms (GA) has recently attracted the attention of researchers in the field of artificial intelligence. From the literature, it is clearly seen that genetic algorithms can provide powerful tools for optimization [15-19]. Genetic algorithms are used as parameter search techniques, which utilize genetic operators to find near optimal solutions. The advantage of a GA technique is that it is independent of the complexity of the performance index considered. It suffices to specify the objective function and to place finite bounds on the optimized parameters.

In this paper, we apply the Rayleigh-Ritz method [21], [22] combined with GA optimization to design EDRA's with desired characteristics and study the effect of different feed design parameters on their input impedance. A GA is used as a parameter search technique which utilizes the genetic operators to arrive at a design for a dual-band, wide-band, or CP EDRA. To this end, we combine the Rayleigh-Ritz method with GA optimization to reach appropriate dimensions of EDR's. To validate this technique, some examples are given and discussed in the following sections.

## II. ANALYSIS OF EDR

In this section, the three-dimensional wave equation in elliptic cylinder coordinates is first expressed, and its solution for an EDR is then investigated. The geometry of EDR is shown in Fig. 1. The EDR is mounted on a ground plane with  $a$  and  $b$  are the semi-major and semi-minor axes, respectively, and  $h$  is the height of the EDR. Image theory can be immediately applied where the ground plane is replaced by an image portion of the cylinder extending to  $z = -h$ . For a DR with very large

dielectric permittivity, the dielectric air interface can be approximated by a hypothetical perfect magnetic conductor (PMC), which requires that the tangential components of the magnetic field vanish on that surface. Rayleigh-Ritz procedure [21] is used in this section to find cut off frequencies of the structure elliptical cross-section field patterns of the DRA. In elliptical coordinates, the scalar Helmholtz equation can be written as,

$$\frac{2}{f_o^2 (\cosh 2\xi - \cos 2\eta)} \left( \frac{\partial^2}{\partial \xi^2} + \frac{\partial^2}{\partial \eta^2} \right) \begin{Bmatrix} E_z \\ H_z \end{Bmatrix} + (k^2 - k_z^2) \begin{Bmatrix} E_z \\ H_z \end{Bmatrix} = 0 \quad (1)$$

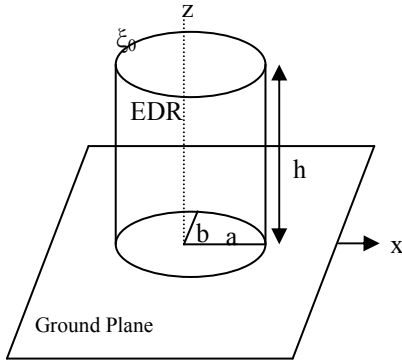


Fig. 1. Schematic diagrams of an EDR.

where  $f_o$  is the semi-focal distance of the ellipse. In order to find  $k_c$  ( $\sqrt{k^2 - k_z^2}$ ) and fields' modes, the Rayleigh-Ritz procedure [21] is employed by minimizing the energy functional of  $X$ ,

$$W(X) = \frac{1}{2} \iint_S \left[ \left( \frac{\partial X}{\partial x} \right)^2 + \left( \frac{\partial X}{\partial y} \right)^2 \right] dx dy - \frac{k_c^2}{2} \iint_S X^2 dx dy \quad (2)$$

with

$$E_z \text{ or } H_z = X \cdot \begin{bmatrix} \sin(k_z z) \\ \cos(k_z z) \end{bmatrix},$$

where  $S$  is the EDRA cross section area. The two-dimensional field,  $X$ , may be expanded as a series of polynomials  $\phi_i$ ,

$$X(x, y) = \sum_{i=1}^m C_i \phi_i \quad (3)$$

where  $C_i$  is constant and  $\phi_i$  is polynomial to be determined later in this section. Therefore, the energy functional of  $X$  is,

$$W(X) =$$

$$\frac{1}{2} \iint_S [C]^T \left[ \left( \frac{\partial \phi}{\partial x} \right) \left( \frac{\partial \phi}{\partial x} \right)^T + \left( \frac{\partial \phi}{\partial y} \right) \left( \frac{\partial \phi}{\partial y} \right)^T \right] [C] dx dy - \frac{k_c^2}{2} \iint_S [C]^T [\phi] [\phi]^T [C] dx dy \quad (4)$$

where  $[C] = [C_1 C_2 C_3 \dots C_m]$  and  $[\phi] = [\phi_1 \phi_2 \phi_3 \dots \phi_m]$ .

Minimizing the energy functional, we obtain

$$[K][C] = k_c^2 [M][C] \quad (5)$$

where the elements in the matrices  $K$  and  $M$  are given by

$$k_{i,j} = \iint_S \left( \frac{\partial \phi_i}{\partial x} \frac{\partial \phi_j}{\partial x} + \frac{\partial \phi_i}{\partial y} \frac{\partial \phi_j}{\partial y} \right) dx dy \quad (6)$$

and

$$m_{i,j} = \iint_S \phi_i \phi_j dx dy \quad (7)$$

The  $i$ -th polynomial,  $\phi_i$ , is defined in terms of a new polynomial  $z_i(x, y)$ . It is generated by the following procedure. Let  $r = \lfloor \sqrt{i-1} \rfloor$ , where the square brackets represent the integer portion of  $t = (i-1) - r^2$ . We define a parameter  $v$  such that,

$$v = t/2; \quad 0 \leq v \leq r; \quad z_i(x, y) = x^r y^v \quad \text{when } t \text{ is even} \quad (8)$$

and

$$v = (t-1)/2; \quad 0 \leq v \leq r-1; \quad \text{when } t \text{ is odd} \quad (9)$$

$$z_i(x, y) = x^v y^r$$

The polynomial  $z_i(x, y)$  has a degree of  $r + v$  and  $\phi_i$  is defined as,

$$TM \text{ Case : } \quad \phi_i(x, y) = z_i(x, y) \quad (10)$$

$$TE \text{ Case : } \quad \phi_i(x, y) = \psi(x, y) z_i(x, y) \quad (11)$$

where  $\psi$  is a constraint function for the elliptical cross-section and given by,

$$\psi = \frac{x^2}{a^2} + \frac{y^2}{b^2} - 1 \quad (12)$$

$\psi$  is added to satisfy the geometrical boundary conditions [21]. In equation (3),  $m$  depends on the order of  $X(x, y)$  and determines the overall accuracy and efficiency of the optimization process. By solving equation (5) for  $k_c$  and

$[C]$ , we obtain solutions for  $E_z$  and  $H_z$  and hence other field components at any point in the resonator. Table 1 shows some resonant frequencies of an EDR and a circular cylindrical dielectric resonator (CDR) with the same height and same cross section area and for different eccentricity ( $e = f_0/a$ ). As shown in the table 1, for the same range of frequency the number of resonant frequencies of EDR is more than the number of resonant frequencies of CDR with the same volume.

Table 1. Resonant frequencies of EDR and CDR with cross section area of  $157\text{mm}^2$  and height of 20 mm (same volume) and permittivity  $\epsilon_r = 12$ .

Mode	$e=f_0/a$	Resonant Frequency (GHz)	
TM110	0 (Circle)	3.748	
TM111		4.840	
TE010		6.051	
TM210		6.494	
TE011		6.781	
TM112		7.547	
TM211		8.046	
TE012		8.144	
TM113		8.260	
TE013		8.809	
Even TM110		0.866	3.371
Even TM210			5.188
Odd TM110			5.334
Even TE010	5.636		
Odd TM210	6.756		
Even TM111	6.990		
Even TM310	7.132		
Even TE110	7.234		
Even TM211	8.026		
Odd TM111	8.121		
Even TE011	8.323		
Odd TM310	8.339		
Even TE020	8.990		
Odd TM211	9.118		
Even TM410	9.245		
Even TM311	9.400		
Even TE111	9.478		
Even TM010	9.572		
Odd TE110	9.684		
Odd TM311	10.346		

Figures 2 and 3 show field contours of the four lowest TM and TE modes for  $b/a=0.75$ , which are calculated using Rayleigh-Ritz method [21]. It is clear that we can obtain more excitation modes for an EDR case compared to a circular one, and also we can control priority order of modes frequencies by changing the axial ratio of the ellipse ( $a/b$ ). Such field distribution patterns may be used to determine the feed location for a special

modes excitation. Mode contour patterns can also be used to recognize paths on which electric or magnetic fields are zero. This allows the study of different EDR portions for different modes. For example, in Fig. 2© there are 2 paths with  $H_z = 0$  with 3 portions of EDR for even  $TE_{02P}$  mode. If wavenumbers of several modes are less than the cutoff wavenumber, then a feeding system can be design such that more than one mode are excited to potentially generate dual-band, circular polarized, or wide-band EDRA's.

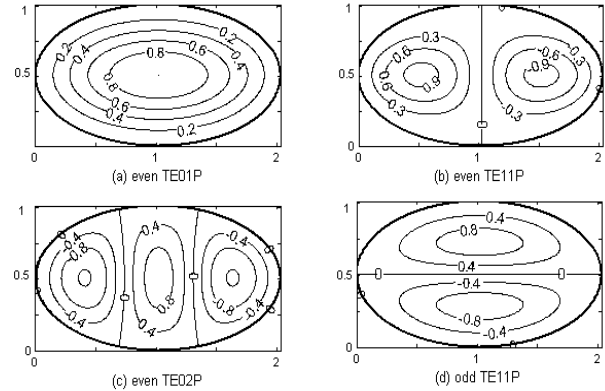


Fig. 2.  $H_z$  Field contour plot of TE modes.

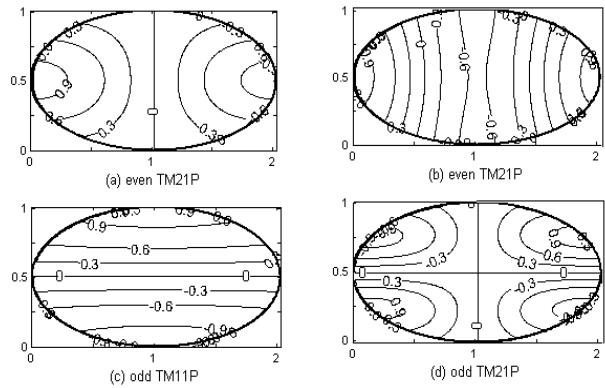


Fig. 3.  $E_z$  Field contour plot of TM modes.

### III. SYNTHESIS OF EDR FOR DESIRED MODES AT A GIVEN FREQUENCY

In short, Genetic Algorithms are search methods based on the principles and concepts of natural selection and evolution [22-25]. These optimization methods operate on a group of trial solutions in parallel, and they operate on the coding of the function parameters rather than the parameters directly. In a Genetic Algorithm, four operators are usually used: cross over, mutation, elitism and selection to make a new population from previous one. The single-point crossover, which is the simplest form and also the best in our case, was used in our

algorithm. In this combination form, genetic information (bits) of two parent chromosomes which are chosen with probability  $P_x$  from the current population are exchanged from a random bit through their ends to form two new children. In order to perform a mutation operator, a chromosome is randomly chosen with probability  $P_m$  and one of its genes (bits) changes. Mutation is generally considered to be a background operator that ensures the probability of searching a particular subspace of the problem space, which is never zero. This has the effect of tending to inhibit the possibility of converging to a local optimum, rather than the global one. After crossover and mutation, the individual strings are selected according to their fitness to form a new generation. To ensure that the best individual of each population survives, we use elitism operator and transfer the fittest chromosome to the next generation. This process continues through subsequent generations and the average performance of individuals in a population is expected to increase, as good individuals are preserved and bred with one another and the less fit individuals die out. The GA used in this paper is terminated either when the fitness function of the best chromosome meets a predefined desired threshold or the number of generations exceeds a predefined maximum.

Resonant modes and frequencies of an EDRA are dependent on EDR dimensions, therefore dimensions of elliptical cross-section are the most important parameters to control resonant frequencies of an EDRA. In this study, the problem is defined in terms of choosing the geometric parameters  $a$  and  $b$  in such a way that the two elements of the eigenvector, obtained using Rayleigh-Ritz technique, have the desired values. To do this, first we define an appropriate encoding scheme that maps each set of feasible parameters to a bit stream. The encoding scheme is very simple: all parameters change to binary values. Using this encoding scheme, we randomly produce bit streams or chromosomes that make the first generation. In other words, each chromosome of this first population has the information of the parameters to be found. The next step is to apply the fitness function to each chromosome of the population. The fitness function for each chromosome is defined as the MSE difference between the eigenvector elements related to parameters obtained from that chromosome and the desired values of those eigenvector elements. Better individuals who have the higher fitness value have higher chances to survive according to the selection operator applied to the population. By applying cross over, mutation, elitism and selection operators to the population, the next generations are produced successively. The optimization process is shown step by step in Fig. 4. The seed chromosome is used to formulate a population of random chromosomes (parents) for simulation in the Rayleigh-Ritz procedure. The priority of primary modes can be approximately determined by the following formulas,

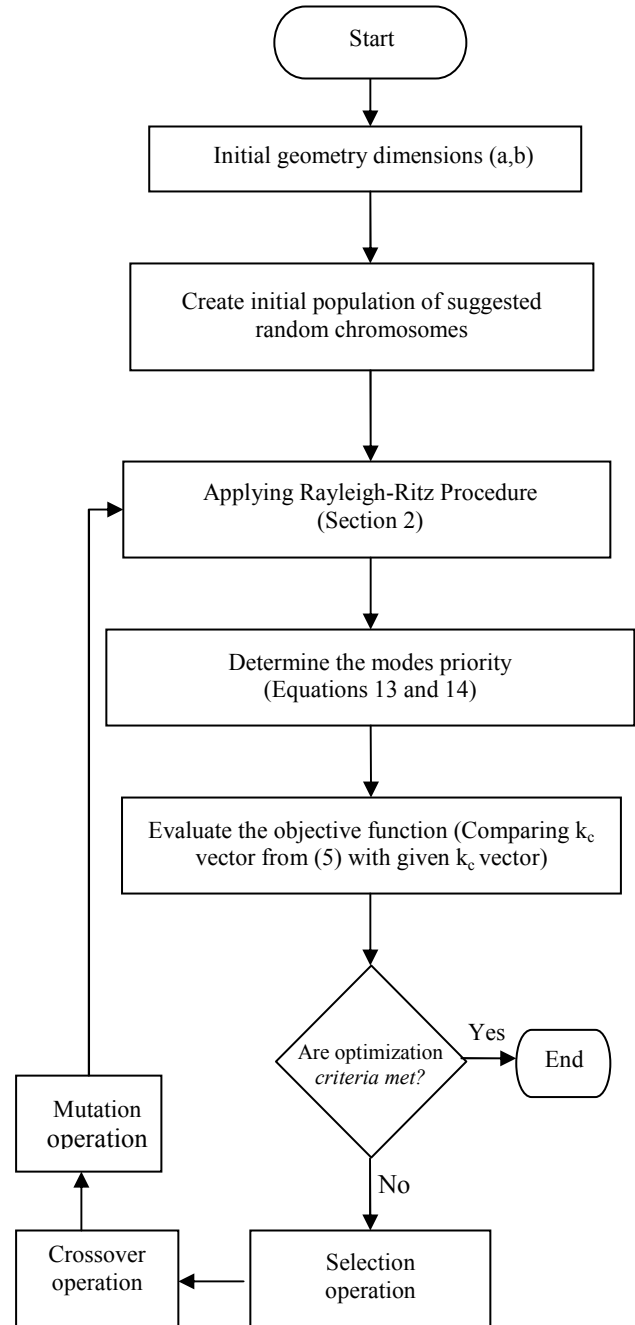


Fig. 4. Flowchart of Genetic Algorithm.

$$TE : \left[ \frac{(2m+1)}{2a} \right]^2 + \left[ \frac{(2n+1)}{2b} \right]^2 \rightarrow P_{mn}^{TE} \quad (13)$$

$$TM : \left[ \frac{m}{a} \right]^2 + \left[ \frac{n}{b} \right]^2 \rightarrow P_{mn}^{TM} \quad (14)$$

where  $P_{mn}^{TE}$  and  $P_{mn}^{TM}$  are notations for the priority of the

TE and TM  $mn^{\text{th}}$  modes, respectively. If the resonant frequency of one mode is smaller than the resonant frequency of another mode, then the priority of that mode is also smaller. For TE and TM modes,  $m$  and  $n$ , respectively, denote the number of contour lines valued zero in the contour plot in  $a$  ( $x$ ) and  $b$  ( $y$ ) directions (Figs. 2 and 3). The resulting mode frequencies for each geometry are obtained by the Rayleigh-Ritz procedure. If the GA converges on the target, the GA process is terminated. The selection operation determines the number of trials for which a particular chromosome (parent) is chosen for reproduction from the created population. The GA keeps looping by creating new generations until it converges to an optimum solution.

A population is created with a group of individuals created randomly in a define range. It can be seen from equations (13) and (14) for different values of  $a$  and  $b$ , the priority of primary modes changes. But this priority does not change for ranges of  $a$  and  $b$  which can be obtained by equations (13) and (14). If two best fitness of the population stock for 100 successive iterations and the objective function was not satisfied then we switch to another ranges of  $a$  and  $b$  with different priority of primary modes. The evaluation function (fitness) gives the individuals a score based on how well they perform at the given task. For the given ranges of  $a$  and  $b$  the objective vector and fitness function are defined as follow,

$$k_m = f_1 \text{ and } k_n = f_2 \Rightarrow \text{Objective Vector} = \begin{bmatrix} k_1 \\ \vdots \\ k_m = f_1 \\ \vdots \\ k_n = f_2 \\ \vdots \end{bmatrix} \quad (15)$$

$$\text{EigenVector of an Individual} = \begin{bmatrix} k_{10} \\ \vdots \\ k_{m0} \\ \vdots \\ k_{n0} \\ \vdots \end{bmatrix} \quad (16)$$

$$\Downarrow$$

$$\text{Fitness} = (f_1 - k_{m0})^2 + (f_2 - k_{n0})^2$$

This continues until a suitable solution has been found or a certain number of generations have passed. In roulette wheel selection, individuals are given a probability of being selected that is directly proportionate to their fitness.

#### IV. APPLICATION OF GA TO DESIGN EDRA WITH GIVEN CHARACTERISTICS

Having control over excitation modes' frequencies gives us a flexibility to achieve certain design requirements or given characteristics. For example, an EDRA can be designed such that it has two desired resonant modes close to given frequencies to generate CP wave at those frequencies, and so on. Designing multi-band, wide-band or circularly polarized antennas is remarkably simple using this method. The previously described hybrid technique, i.e. GA and Rayleigh-Ritz procedure, is applied to EDRs. Figure 5 shows the geometry of an offset slot-coupled EDRA fed by microstrip line. The finite ground plane with an etched slot is located on the top of the surface of a substrate. To examine this issue, some examples to show different slot-coupled EDRA are presented and discussed in the following sub-sections. Mode patterns presented in Figs. 2 and 3 lead us to locate the feeding system to excite two desired modes.

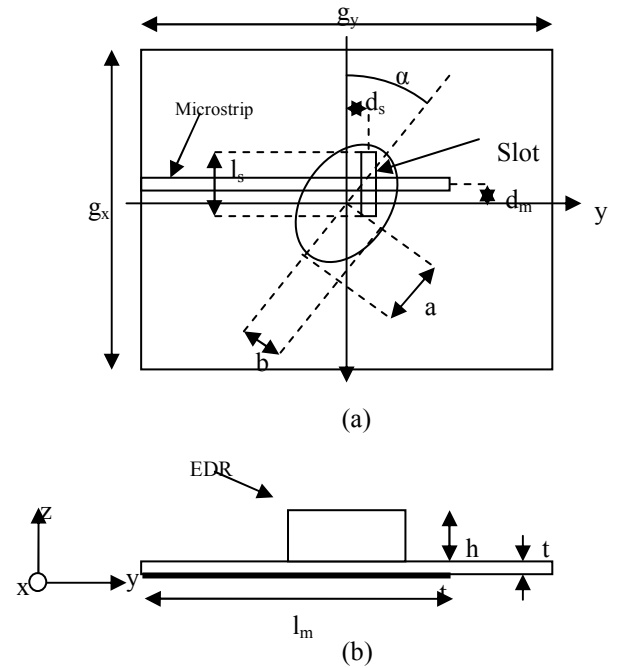


Fig. 5. Schematic diagrams of the proposed EDRA. (a) Top view. (b) Side view.

##### A. Dual-Band EDRA

Dual band operation of DRAs may be obtained by proper excitation of the DR. Consider an EDRA with a required dual-band operation at 2.5 and 4 GHz. The GA is applied in order to obtain  $a$  and  $b$ .

We set two different modes (for example here we chose odd  $TM_{210}$  and even  $TM_{310}$ ) at 2.5GHz and 4GHz. To compensate for the PEC approximation to calculate

fields of the EDRA, the size of the slot and its position with respect to the EDR can be tuned. We fixed the values of  $h=26\text{mm}$ ,  $l_m=22\text{mm}$ ,  $l_s=24\text{mm}$ ,  $w_s=1.2\text{mm}$ ,  $\alpha=23^\circ$ ,  $g_x=g_y=80\text{mm}$ ,  $t=1.5\text{mm}$  and obtained suitable DR dimensions based on GA:  $a=13.37\text{mm}$ , and  $b=16.49\text{mm}$ . Figure 6 illustrates the magnitude of the return loss of the offset slot-coupled EDRA. By applying GA, the simulated center frequencies are 2.48GHz and 4.03GHz. Ansoft-HFSS [27] simulations with optimizing size and position of slot, give mode resonant frequencies 2.51 and 4.00GHz, respectively. Figures 7 and 8 plot the simulated radiation patterns at 2.5 and 4GHz in the y-z and x-z planes. From these results, the patterns are similar to those radiated by a horizontal magnetic dipole at these two frequencies.

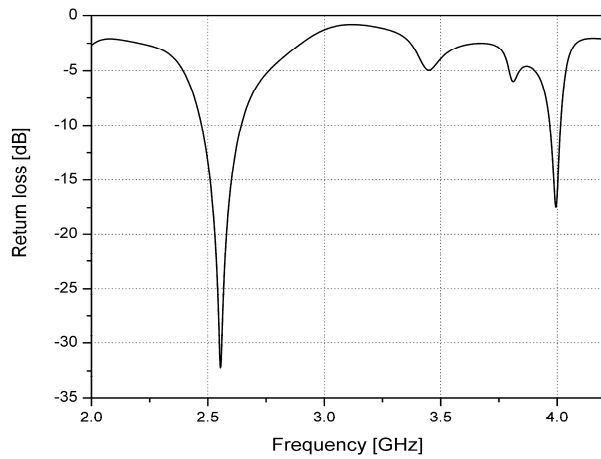


Fig. 6. Return Loss of the Designed Dual-Band EDRA.

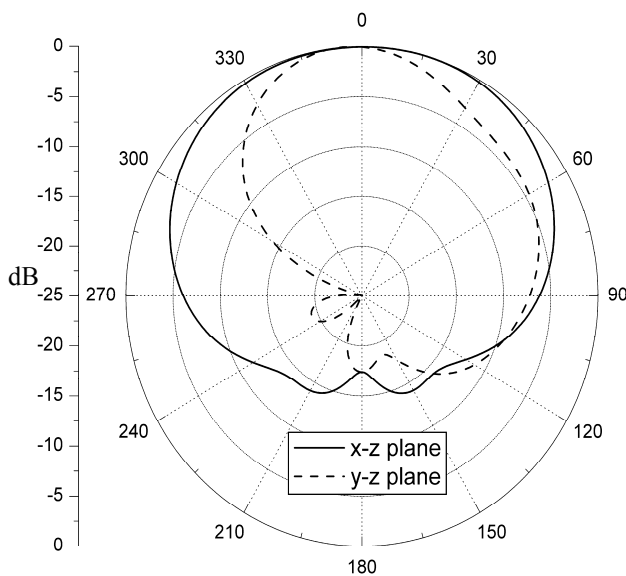


Fig. 7. Far Field Pattern of the EDRA at 2.5 GHz.

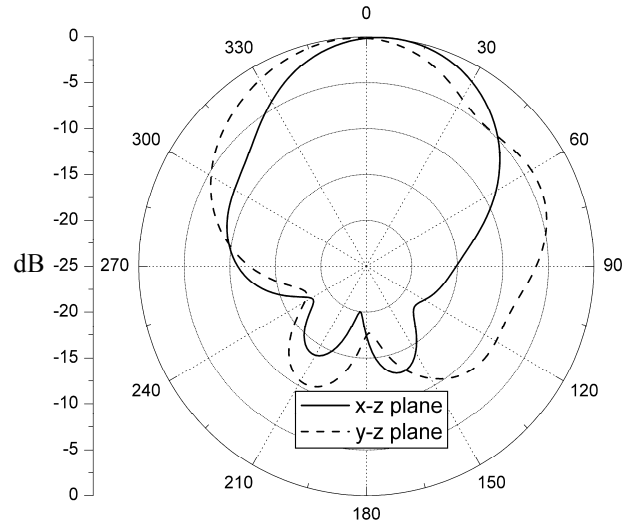


Fig. 8. Far Field Pattern of the EDRA at 4 GHz.

### B. Wide-Band EDRA

In this example, we discuss the design of a wideband slot-fed EDRA at 2.9GHz. Using the proposed GA, the second and eighth modes were set at 2.7 and 3.1GHz, respectively. Varying the slot offset has some effect on the resonant frequencies of the excited modes. Figure 9 shows the simulated return loss as a function of frequency for an EDRA after GA and feed tuning were used. A bandwidth of 21.7% around 2.9GHz is achieved. The optimized parameters are  $h=30\text{mm}$ ,  $l_m=25\text{mm}$ ,  $l_s=18\text{mm}$ ,  $w_s=1.5\text{mm}$ ,  $\alpha=17^\circ$ ,  $a=15.02\text{mm}$ ,  $b=19.53\text{mm}$ ,  $g_x=g_y=80\text{mm}$ , and  $t=1.5\text{mm}$ . The radiation patterns of the proposed antenna in both x-z and y-z planes were simulated at 2.70, 2.90, and 3.10 GHz, and are shown in Figs. 10 to 12. As shown in Figs. 10 to 12, variation of far field patterns is not too much over the band.

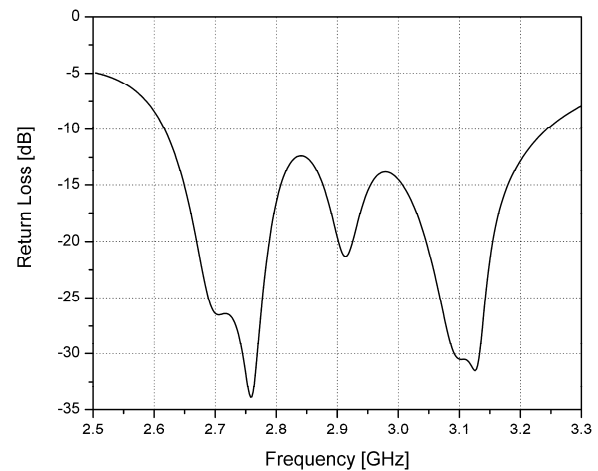


Fig. 9. Return Loss of the Designed Wide-Band EDRA

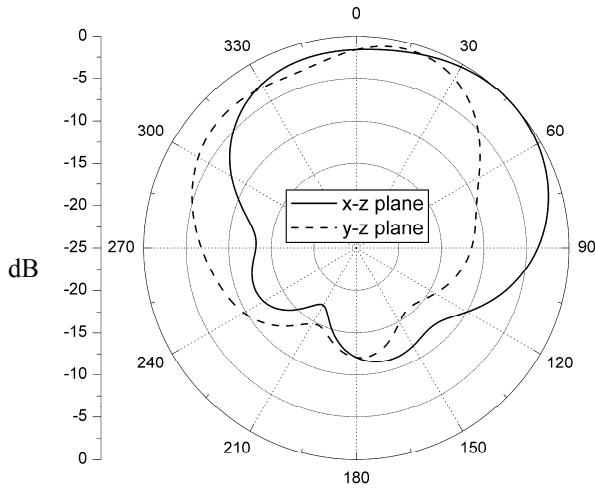


Fig. 10. Far Field Pattern of the EDRA at 2.7 GHz.

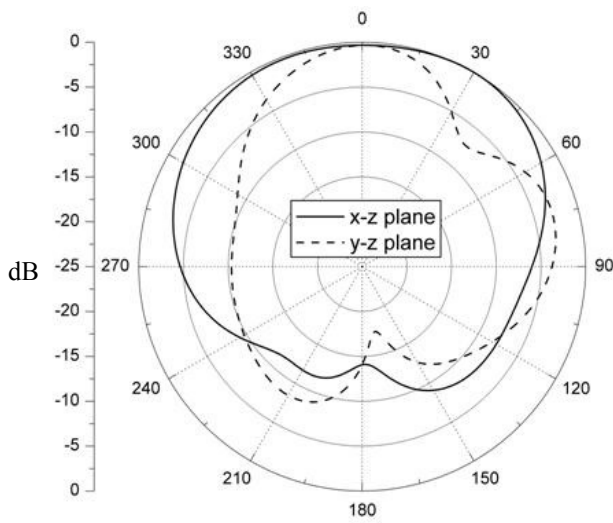


Fig. 11. Far Field Pattern of the EDRA at 2.9 GHz.

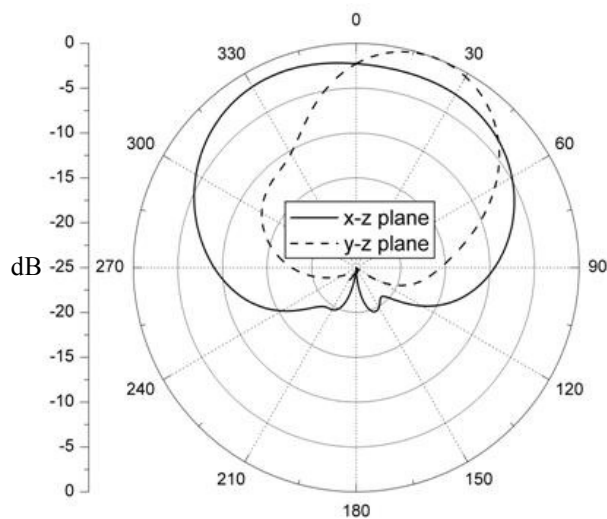


Fig. 12. Far Field Pattern of the EDRA at 3.1 GHz

**C. Circularly Polarized EDRA**

Recently, the circularly polarized (CP) DRA has received increasing attention because of its insensitivity to antenna orientation between the transmitter and receiver, which is very useful in satellite communications. Quadrature feeds and special DRAs have often been used for CP DRA design. However, the former increases the size and complexity of the feed network, whereas the latter is not easily available on the commercial market. Recently, most CP DRA work has concentrated on a single feed using normal DRAs. In this third example, we focus on the design of a CP DRA at 3 GHz. Applying GA, we set even  $TE_{020}$  mode at 2.95GHz and odd  $TE_{110}$  mode at 3.05GHz. Similar to the two previous sections, by tuning the slot size and its position, good results are obtained for an EDRA with  $h=29\text{mm}$ ,  $l_m=25\text{mm}$ ,  $l_s=18\text{mm}$ ,  $w_s=1.5\text{mm}$ ,  $\alpha=15^\circ$ ,  $a=14.97\text{mm}$ ,  $b=20.96\text{mm}$ ,  $g_x=g_y=80\text{mm}$ , and  $t=1.5\text{mm}$ . Figure 13 shows the return loss versus frequency. Figure 14 shows the corresponding axial ratio (AR). From these results, it is observed that the -3dB AR bandwidth is 2.7%, which is reasonable for a single-fed CP EDRA. The simulated x-z and y-z plane radiation patterns at 3.03GHz are displayed in Fig. 15, where broadside field patterns are observed, as expected.

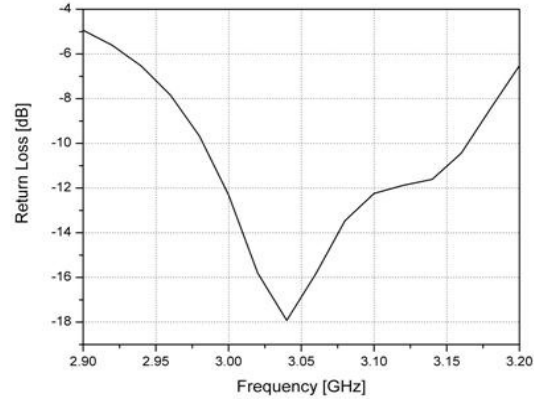


Fig. 13. Return Loss of the Designed Circular polarized EDRA.

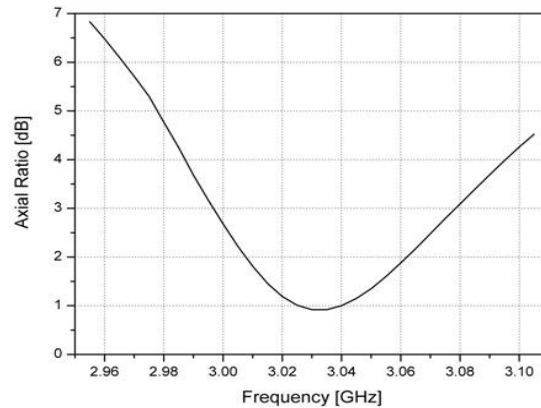


Fig. 14. Axial Ratio of The EDRA at  $\theta=0^\circ$ .

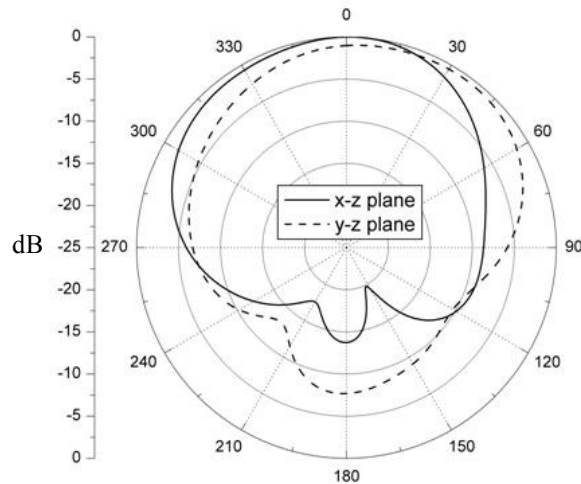


Fig. 15. Far Field Pattern of the EDRA at 3.03 GHz.

## V. CONCLUSION

In this paper, a genetic algorithm has been introduced and presented for numerical optimization to obtain suitable dimensions of an EDRA with resonant modes at specified frequencies. The Rayleigh-Ritz method together with GA is used to calculate minor and major radii of the ellipse. Since each element of the calculated eigenvector using the Rayleigh-Ritz technique related to a mode frequency, we can require that a particular mode become excited at a certain frequency. Therefore, this technique is used to design EDRA with desired characteristics. Examples are given to demonstrate the design of a dual band EDRA at two desired frequencies, and a wide band EDRA with 21.7% bandwidth at a given centered frequency. Also, an example is presented to show a single fed EDRA with two resonant modes close to each other to generate CP with 2.7% CP bandwidth. This paper illustrates that EDRA is a good candidate for a small antenna with wide range of given antenna characteristics including circular polarization, wide-band and dual-band operation.

## REFERENCES

- [1] R. K. Mongia and P. Bhartia, "Dielectric resonator antennas—A review and general design relations for resonant frequency and bandwidth," *Int. J. Microwave Millimeter-Wave Eng.*, vol. 4, pp. 230–247, July 1994.
- [2] R. K. Mongia, A. Ittipiboon, and M. Cuhaci, "Measurement of radiation efficiency of dielectric resonator antennas," *IEEE Microwave Guided Wave Lett.*, vol. 4, pp. 80–82, Mar. 1994.
- [3] A. Petosa, A. Ittipiboon, Y. M. M. Antar, D. Roscoe, and M. Cuhaci, "Recent advances in dielectric resonator antenna technology," *IEEE Antennas Propagat. Mag.*, vol. 40, pp. 35–48, June 1998.
- [4] S. A. Long, M. McAllister, and L. C. Shen, "The resonant cylindrical cavity antenna," *IEEE Trans. Antennas Propagat.*, vol. AP-31, pp. 406–412, May 1983.
- [5] M. McAllister, S. A. Long, and G. L. Conway, "Rectangular dielectric resonator antenna," *Electron. Lett.*, vol. 19, pp. 219–220, Mar. 1983.
- [6] M. Young, *The Technical Writers Handbook*. Mill Valley, CA: University Science, 1989.
- [7] M. McAllister and S. A. Long, "Resonant hemispherical dielectric antenna," *Electron. Lett.*, vol. 20, pp. 657–659, Aug. 1984.
- [8] K. W. Leung, K. M. Luk, K. Y. A. Lai, and D. Lin, "Theory and experiment of a coaxial probe fed hemispherical dielectric resonator antenna," *IEEE Trans. Antennas Propagat.*, vol. 41, pp. 1390–1398, Oct. 1993.
- [9] R. K. Mongia, A. Ittipiboon, P. Bhartia, and M. Cuhaci, "Electric monopole antenna using a dielectric ring resonator," *Electron. Lett.*, vol. 29, pp. 1530–1531, Aug. 1993.
- [10] R. K. Mongia, A. Ittipiboon, M. Cuhaci, and D. Roscoe, "Circularly polarized dielectric resonator antenna," *Electron. Lett.*, vol. 30, pp. 1361–1362, Aug. 1994.
- [11] Y. M. M. Antar and Z. Fan, "Characteristics of aperture coupled rectangular dielectric resonator antenna," *Electron. Lett.*, vol. 31, pp. 1209–1210, July 1995.
- [12] S. M. Shum and K. M. Luk, "Analysis of aperture coupled rectangular dielectric resonator antenna," *Electron. Lett.*, vol. 30, pp. 1726–1727, Oct. 1994.
- [13] T. B. Ng, Y. O. Yam, and M. L. Lam, "Active quarter-wavelength dielectric radiator with circularly polarized radiation pattern," *Electron. Lett.*, vol. 27, pp. 1758–1759, 1991.
- [14] G. D. Loos and Y. M. M. Antar, "A new aperture-coupled rectangular dielectric resonator antenna array," *Microwave Opt. Tech. Lett.*, vol. 7, pp. 677–678, 1994.
- [15] A. Tadjalli, A. R. Sebak, T. A. Denidni, A. A. Kishk, "Spheroidal dielectric resonator antenna," *URSI Digist, 2004 USNC/URSI National Radio Science Meeting*, p. 184, 2004.
- [16] R. Fletcher, *Practical Methods of Optimization*. Chichester, U.K.: Wiley Intersci., 1980.
- [17] L. C. W. Dixon, *Global Optima Without Convexity*, in *Design and Implementation of Optimization Software*. Sijnoof Noordhof, The Netherlands: Aalphen aan den Rijn, 1978.
- [18] L. Davis, *Genetic Algorithms and Simulated Annealing*. London, U.K.: Pittman, 1987.
- [19] K. A. DeJong, An analysis of the behavior of a class of genetic adaptive systems, Ph.D. dissertation, Univ. Michigan, 1975.
- [20] D. E. Goldberg, *Genetic Algorithms in Search, Optimization and Machine Learning*. Reading, MA: Addison-Wesley, 1989.
- [21] A. Tadjalli, A. R. Sebak and T. Denidni, "Elliptical Cylinder Dielectric Resonator Antenna," *ANTEM International Symposium*, Ottawa, Aug. 2004.
- [22] B. Singh and D. K. Tyagi, "Transverse vibrations of an elliptic plate with variable thickness," *J. Sound Vib.*, vol. 99, no. 3, pp. 370–391, 1985.
- [23] R. L. Haupt, "An Introduction to Genetic Algorithms for Electromagnetics," *IEEE Antennas and Propagation Magazine*, vol. 37, no. 2, pp. 7–15, April 1995.
- [24] J. M. Johnson, Y. Rahat-Samii, "Genetic Algorithms in Engineering Electromagnetics," *IEEE Antennas and Propagation Magazine*, vol. 39, no. 4, pp. 7–21, Aug. 1997.
- [25] J. M. Johnson, Y. Rahat-Samii, "Genetic Algorithm Optimization and its Application to Antenna Design," *IEEE Antennas and Propagation Society International Symposium Digest*, vol. 1, pp. 326–329, Jun 1994.
- [26] B. Orchard, "Optimising Algorithms for Antenna Design," MSc Dissertation, University of the Witwatersrand, 2002.
- [27] Ansoft HFSS v.9.2.1, Ansoft Corporation, Pittsburgh, PA 15219-1119, USA.